

Condensation/Hydrogenation of Biomass-Derived Oxygenates in Water/Oil Emulsions Stabilized by Nanohybrid Catalysts

Paula A. Zapata · Jimmy Faria · M. Pilar Ruiz · Daniel E. Resasco

Published online: 22 February 2012
© Springer Science+Business Media, LLC 2012

Abstract The synthesis of fuel-range molecules by condensation of biomass-derived furfural and acetone has been studied in a biphasic emulsion system. Nanohybrids composed of basic oxide nanoparticles fused to carbon nanotubes have been used to simultaneously stabilize water/oil emulsions and catalyze the condensation reaction. Under the same conditions, higher conversions and higher fractions of fuel-range condensation products (C₈–C₁₃) have been obtained in the emulsion compared to those obtained in the single phase. Furthermore, when using metallized nanohybrids these emulsions have been used to hydrogenate the oil-soluble condensation products. Both model compounds and synthetic bio-oil mixtures have been used to demonstrate that catalytic emulsion systems could be effective for upgrading complex mixtures, such as pyrolysis oil.

Keywords Carbon nanotubes · Nanohybrids · Hydrophobic and hydrophilic catalysts · Emulsion · Aldol-condensation · Hydrogenation · Oxygenates · Pyrolysis oil · Bio-oil

Electronic supplementary material The online version of this article (doi:10.1007/s11244-012-9768-4) contains supplementary material, which is available to authorized users.

P. A. Zapata · J. Faria · M. Pilar Ruiz · D. E. Resasco (✉)
School of Chemical, Biological and Materials Engineering,
Center of Interfacial Reaction Engineering, University
of Oklahoma, Norman, OK 73019, USA
e-mail: resasco@ou.edu

P. A. Zapata
e-mail: paula.a.zapata@ou.edu

J. Faria
e-mail: jimmy.faria@ou.edu

M. Pilar Ruiz
e-mail: maria.p.ruiz-2@ou.edu

1 Introduction

The conversion of biomass-derived compounds to transportation fuels may result in important environmental, economic, and strategic advantages. It is particularly desirable to produce liquids that can be fungible with conventional fuels [1–3]. The target products are low-oxygen, high-energy-content liquids, which should be produced in a large-scale process with enough versatility to accept different kinds of biomass feedstocks [4, 5]. Several primary biomass conversion technologies have been investigated during the last few years, including acid hydrolysis, gasification, indirect liquefaction, and pyrolysis, which produce sugars, dehydrated sugars, syngas, and pyrolysis oils that need to be upgraded in subsequent steps [6–10]. In general, studies of upgrading strategies have addressed the primary conversion products of each of the technologies individually, which often limits the possibility of fully utilizing intermediates and products.

An example of effective process integration would be the condensation of furfurals with short ketones, such as acetone, which can be readily obtained by ketonization of acetic acid, one of the major components in the aqueous fraction of pyrolysis oil. In turn, furfural is produced by dehydration of sugars, from either hydrolysis of cellulose or pyrolysis of ligno-cellulosic biomass. Therefore, one can envision a reaction system that combines acetone (from pyrolysis) and furfurals (from hydrolysis and/or pyrolysis). Small ketones can act as effective linkers of furfural to produce larger hydrocarbon molecules (C₈–C₁₃), which fall in the gasoline/diesel range.

Condensation reactions of furan-derived compounds with ketones and aldehydes can be conducted in both monophasic and biphasic systems [11–20]. For instance, Dumesic et al. [14] used a bifunctional catalyst

(Pd/MgO–ZrO₂) in a single aqueous phase reactor to perform aldol-condensation of furfural and 5-hydroxymethyl-furfural (HMF) with acetone. After the aldol-condensation step, the products were dissolved in hexadecane and subjected to hydrogenation. In a subsequent study [15], they conducted the condensation of furfural and HMF with acetone in aqueous phase, using NaOH as a catalyst. The condensation products were readily separated by putting them in contact with an organic phase and adding NaCl to the aqueous solution. Unfortunately, the limited solubility of furfural in water made it necessary to use high amounts of base to observe substantial activity. Likewise, Huber et al. [16] compared the performance of MgO–ZrO₂, NaY, and ammine-substituted NaY zeolites as catalysts for the condensation of furfural (C₅) with acetone and propanal (C₃). They observed that MgO–ZrO₂ resulted in higher selectivity to double aldol-condensation with a ratio of 4-(2-furyl)-3-buten-2-one (C₈) to 1,5-bis-(2-furanyl)-1,4-pentadien-3-one (C₁₃) of 0.8, while NaY and ammine-NaY gave better selectivity to the C₈ product with ratios of C₈ to C₁₃ of 2.2 and 9, respectively. The higher molecular weight products obtained through aldol-condensation followed by hydrogenation could be used directly as current fuel additives or alternative fuels [21, 22].

The use of a biphasic system in this type of reactions may become a technological advantage since the components of bio-oil (catechols, syringols, guaiacols, phenolics, sugars, ketones, aldehydes, short carboxylic acids, and furfurals) have different solubilities in water and oil [23]. The water content in bio-oil is about 40% [24, 25], and when it is contacted with hydrocarbons or with partially deoxygenated fractions of the same bio-oil, a phase separation occurs, with a corresponding product distribution that depends on the partition coefficient of the compounds. Therefore, if properly handled, the presence of the two phases could be advantageously used in a reactive separation scheme in a continuous process.

In this context, we have recently shown that reactions taking place at the water/oil interface in emulsions stabilized by nanohybrid catalysts composed of functionalized carbon nanotubes (CNT) fused to metal oxides offer several advantages. For example, the enhanced interfacial area favors the rate of mass transfer between the two phases. Also, molecules preferentially present in one of the phases can be selectively converted in that phase by proper location of the catalytically active species. Finally, the continuous reaction and separation of products, based on their relative solubilities can be efficiently combined [26–29]. The amphiphilic character of these nanohybrids derives from the hydrophobicity of the CNT [30, 31] combined with the hydrophilicity of the metal oxides [32–34] used as catalyst support to grow the nanotubes. We have shown that this amphiphilic character makes them suitable to

stabilize Pickering emulsions in water/oil systems [27]. By fine tuning the composition of the nanohybrids, it is possible to tailor the emulsion properties (volume, droplet size, emulsion type), the metal dispersion and location and, therefore, the resulting product distribution [28].

After promising results obtained in the initial applications of this novel technology [26–29, 31], we report here the simultaneous condensation and hydrogenation of short biomass-derived oxygenates in emulsions stabilized by catalytic nanohybrids.

2 Experimental

2.1 Nanohybrid Catalyst Preparation and Characterization

Different nanohybrids were synthesized to be used as catalysts for the different reactions performed. For aldol-condensation reactions, nanohybrids composed of CNT grown on basic metal oxides were used, whereas for hydrogenation reactions, metal clusters (Pd, Pt, Ni) were anchored on the nanohybrids.

2.1.1 CNT/Basic Oxide Nanohybrid Catalysts

For the aldol-condensation reactions, a basic catalyst is usually needed. Thus, several nanohybrids composed of CNT grown on different basic metal oxides were prepared and their activities for the aldol-condensation of furfural and acetone were compared. Several basic metal oxides were chosen: MgO, ZnO, TiO₂ and Mg–Al, and Ce–Zr mixed oxides.

- (a) *SWCNT and MWCNT/MgO*. In these nanohybrids, the CNT were grown on the same MgO-based catalyst. Depending on the type of gas and conditions used, it is possible to selectively grow either single-wall (SWCNT) or multi-wall (MWCNT) CNT. The initial catalyst for CNT growth was prepared by a combustion method in which a solution of the precursors, Mg(NO₃)₂·6H₂O, Fe(NO₃)₃·9H₂O and (NH₄)₆Mo₇O₂₄·4H₂O (Sigma Aldrich), was mixed with citric acid (Sigma Aldrich) used as combustible agent, and then calcined at 500 °C for 2 h. The total metal loading (Fe and Mo) was 4 wt% with a molar ratio Fe:Mo of 10:1. In order to grow SWCNT, this catalyst was first reduced under 200 sccm of H₂ at 500 °C for 30 min, then heated in 200 sccm of He up to 850 °C, and finally exposed to a flow of 200 sccm of 3% of CH₄ in He at this temperature for 1 h. The total carbon yield obtained from this reaction was around 16 wt%. To obtain MWCNT, the same initial catalyst was first reduced under 300 sccm of H₂ at 500 °C for 30 min, then heated in 300 sccm of He up to 700 °C, and

finally exposed to a flow of 400 sccm of 25% of C_2H_4 in He at this temperature for 20 min. The total carbon yield obtained from this reaction was ~ 36 wt%.

- (b) *MWCNT/MgO₂Al₂O₃*. The MgO/Al₂O₃-based catalyst was synthesized by the same combustion method explained above. A solution of the precursors, Mg(NO₃)₂·6H₂O, Fe(NO₃)₃·9H₂O, (NH₄)₆Mo₇O₂₄·4H₂O, and Al(NO₃)₃·9H₂O (Sigma Aldrich), was mixed with citric acid (combustible agent) and then calcined at 500 °C for 2 h. The total metal loading (Fe and Mo) was 4 wt% with a molar ratio Fe:Mo:Mg:Al of 1:0.1:16:7. The MWCNT were grown on this catalyst following the same procedure to grow MWCNT on the MgO catalyst.
- (c) *MWCNT/Ce_xZr_{1-x}O₂, V₂O₅, ZnO, and TiO₂*. The vanadium, zinc, and titanium oxides were provided by Sigma Aldrich. The cerium-zirconium mixed oxide (Ce_xZr_{1-x}O₂) was prepared by precipitation, using aqueous solutions of cerium (IV) ammonium nitrate and zirconium nitrate, as previously described [35–37]. Each support was impregnated at incipient wetness with an aqueous solution of Co(NO₃)₂·6H₂O and Fe(NO₃)₃·9H₂O (Sigma Aldrich), at a Fe:Co molar ratio of 2:1, with a final metal loading of 2 wt%. The impregnated powder was dried overnight at 100 °C and calcined in air at 450 °C for 2 h. After cooling, 0.3 g of powder was placed in a tubular reactor, reduced under 300 sccm of H₂ at 500 °C for 30 min, heated to 700 °C in 300 sccm flow of He, and finally exposed at the same temperature to a 400 sccm flow of 25% C₂H₄ in He at 700 °C for 30 min.

2.1.2 Metallized Nanohybrid Catalysts

In order to perform the hydrogenation of the aldol-condensation products, three different nanohybrid-supported catalysts were tested: (a) a physical mixture of SWCNT/MgO and Pd/SWCNT, (b) Pd/MWCNT₂Al₂O₃, and (c) Pt/MWCNT₂Al₂O₃.

- (a) *Physical mixture of SWCNT/MgO and Pd/SWCNT*. In order to perform the hydrogenation of the aldol-condensation products, a catalyst was prepared by a physical mixture (wt. ratio 2:1) of metal-free SWCNT/MgO and pure SWCNT (MgO-free) doped with 10 wt% Pd. To deposit Pd, purified SWCNT provided by SouthWest NanoTechnologies Inc. were sonicated for 15 min with 20 mL of a solution of Pd(NO₃)₂·6H₂O (Sigma Aldrich) in water. The suspension was then dried in a vacuum oven at 60 °C for 2 days. Finally, the resulting powder was calcined in He at 300 °C for 2 h.
- (b-c) *Pd and Pt/MWCNT₂Al₂O₃*. Nanohybrids consisting of MWCNT fused to Al₂O₃ were provided by

SouthWest NanoTechnologies Inc. These nanohybrids were used as a support of Pd or Pt particles for the hydrogenation reactions. Both metals were anchored by incipient wetness impregnation of the aqueous solutions of their corresponding precursors (Pd(NO₃)₂·6H₂O or H₂PtCl₆·6H₂O, respectively). The final metal loading was 5 wt% of Pd or Pt, respectively. After the impregnation, the catalysts were dried overnight at 100 °C and calcined at 300 °C for 2 h in He.

2.2 Reaction Systems

The catalytic experiments of aldol-condensation and hydrogenation were carried out in two Parr 4843 reactors (volumes: 50 and 300 mL). The temperature inside the reactor was measured with a J-Type thermocouple (OMEGA) and controlled by a temperature controller CAL 9500P from CAL Controls Ltd. In each reaction run, the catalyst was dispersed in a mixture of equal volumes of deionized water/decalin and sonicated for 15 min with a horn sonicator (Fisher Scientific 600 W, 20 kHz) at 25% of amplitude. The mixture was placed in the stainless steel reaction vessel and purged with a 200 sccm flow of N₂ for 1 h, while stirring at 200 rpm. Then, the pressure and temperature were raised to the desired operating set points. Finally, the reactants were transferred to the reactor from the feeding cylinder, which was pressurized with N₂ at 50 psig above the reactor pressure.

2.2.1 Aldol-Condensation Reactions

For the aldol-condensation reaction, the flow of N₂ was stopped at the desired pressure (300–400 psi) and the reactant mixture was injected, operating the reactor in the batch mode. The aldol-condensation reactions were performed at 80 and 100 °C when solid nanohybrid catalysts were used, and 40 °C when NaOH was used as a homogeneous catalyst. For the latter, NaOH was dissolved in deionized water and mixed with decalin in a volume ratio 1:1 at a concentration of 0.05 mol NaOH/mol furfural. Then, MWCNT/Al₂O₃ nanohybrids were added to stabilize the emulsion, which was formed upon 15 min sonication with a horn sonicator.

2.2.2 Hydrogenation Reactions

For the hydrogenation step that followed the condensation reactions, the catalyst was pre-reduced in H₂ at 300 psi and 100 °C for 1–3 h. This step was run in semi-batch mode, by flowing H₂ through the system at the desired pressure and temperature conditions (300–900 psi H₂ and 100–230 °C).

After reaction, the emulsion was broken filtering the nanohybrids in two steps. First, a coarse paper filter (8 μm pore) was used to trap a large fraction of the solid nanohybrids since they quickly agglomerate over the surface of the filter. In the second step, a PTFE (0.2 micron pores) filter was used to separate the small fraction of nanohybrids that passed the first filter. The two clear liquid phases obtained after filtration were easily separated and 500 μL samples of each one analyzed by gas chromatography (GC-FID and GC-MS). While the concentration of water in decalin was negligible, decalin was present in water in concentrations lower than around 0.05%. In all the GC-FID analyses, methanol and 1,2-dichloromethane were used as internal standards to help closing the mass balances. All the aqueous fractions were extracted in methanol before injecting them in the GC, to minimize column damage. An Agilent GC-FID 6890A equipped with a capillary column of polyethylene glycol (HP-INNOWAX) of 60.0 m \times 0.32 mm \times 0.25 mm nominal was used for quantitative analysis, while a Shimadzu QP2010S GC-MS equipped with an HP-INNOWAX polyethylene glycol capillary column, 30.0 m long \times 0.25 mm nominal, was used for product identification, by using standards for those compounds that are commercially available.

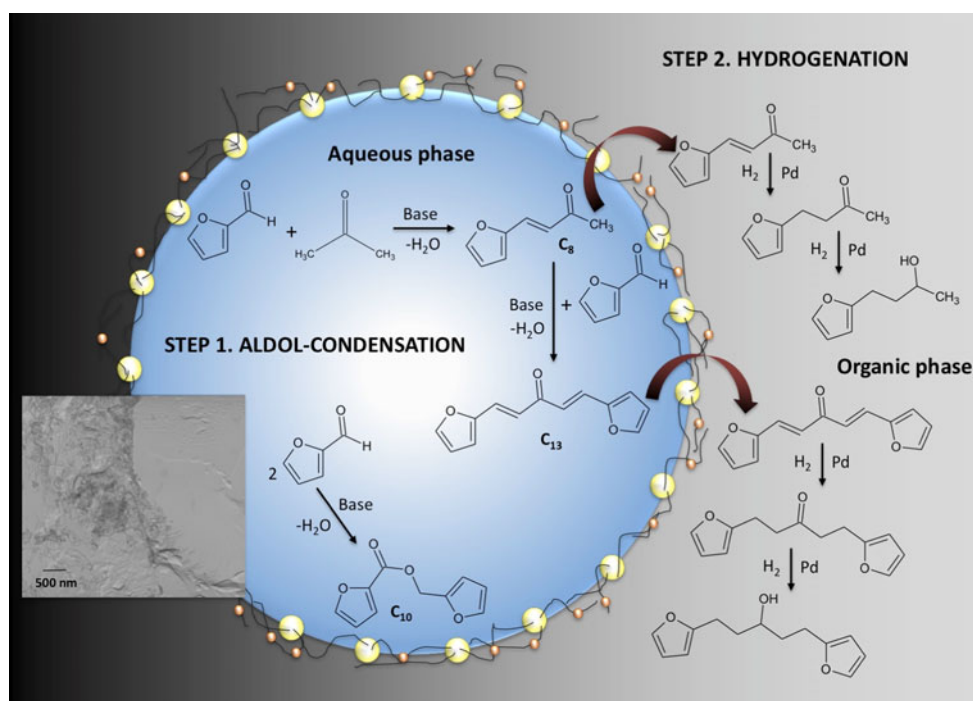
In addition, a quantitative structure–property relationship (QSPR) software was used to predict the relative retention times (RRT) and relative response factors (RRF) of a flame ionization detection (FID) system for the products that are not commercially available. QSPR has been applied to estimate fuel properties such as cetane number

[38, 39], octane number (RON and MON) [40], and sooting tendencies [41] of any fuel component, on the basis of the molecular structure. Other authors have also used QSPR to predict chromatographic factors, using multiple linear regressions and artificial neural networks [42]. In the present work, we have calculated quantum-chemical descriptors and physical properties based on molecular structures of the compounds by using the commercial software QSAR/QSPR MDL. In addition, the boiling point of the compounds obtained from the literature was added to the model descriptors. Multiple linear regressions were done in order to develop QSPR models to predict retention time and relative response factors to the compounds of interest. More detailed information about the QSPR calculations can be found in the supplementary information.

3 Results and Discussion

Figure 1 illustrates the reaction paths and phase migrations involved in the biphasic emulsion upgrading process used in this study. In the first-step, aldol-condensation of furfural and acetone produces compounds in the range C_8 – C_{13} in an emulsion stabilized by nanohybrid catalysts that incorporate a basic oxide catalyst. Once the long-chain products are formed, their solubility in water greatly decreases and they migrate to the organic phase. In the second step, metallized nanohybrids catalyze subsequent hydrogenation reactions, which depending on the degree of severity, partially improve the stability of the product or completely

Fig. 1 Schematic illustration of the aldol-condensation and hydrogenation reactions taking place at the water/oil interface in nanohybrid-stabilized emulsions



eliminate the oxygenated groups. To demonstrate the application of this technology in more complex mixtures relevant to biomass conversion, a few synthetic bio-oils (SBO) have been used as feed for the same tandem of reactions in the emulsion system.

3.1 Nanohybrid Catalyst Characterization

Figure 2 shows the Raman spectrum and the high-resolution transmission electron microscopy (HRTEM) image of the nanohybrids composed of SWCNT and MgO. Raman spectroscopy is widely employed in evaluating the purity and quality of CNT products [43–45]. The relative density of defects in different CNT samples is usually evaluated in terms of two characteristic bands. The G band, at $\sim 1,590\text{ cm}^{-1}$, is ascribed to sp^2 ordered carbon, and the D band, at $\sim 1,350\text{ cm}^{-1}$, is commonly ascribed to sp^3 carbon associated with defects [46–48]. The Raman spectrum corresponding to SWCNT/MgO (Fig. 2 Left) shows a very intense G band and a weak D band. The high G/D intensity ratio, (~ 15) is indicative of CNT with a low density of defects.

Figure 3a shows HRTEM images of MWCNT/MgO nanohybrids. The CNT/oxide mass ratio in these nanohybrids is much higher than in the SWCNT/MgO (compare with Fig. 2). Also, it can be noted that the sample of MWCNT/ZnO (Fig. 3c) has much more defective CNT than the rest of the samples (i.e., the tubes exhibit more kinks and tortuous morphology). As we have shown before [28], the density of defects on the carbon side of the nanohybrids greatly affects the emulsion properties as well as the dispersion of the metal particles. Raman of this sample showed low G/D ratios, indicative of a high defect density.

Figure 4 shows the Raman spectrum of the purified SWCNT together with an HRTEM image of the 10 wt% Pd/purified SWCNT catalyst. While a high intensity G band is observed, the G/D ratio (~ 7) is lower than in the

as-produced material (~ 15). This decrease in the G/D ratio is due to the attack of the SWCNT walls by acids used during the nanotube purification process used to eliminate the catalyst. Some sp^3 carbon defects are created in the surface of the SWCNT, which increases the D band intensity.

3.2 Aldol-Condensation Reactions

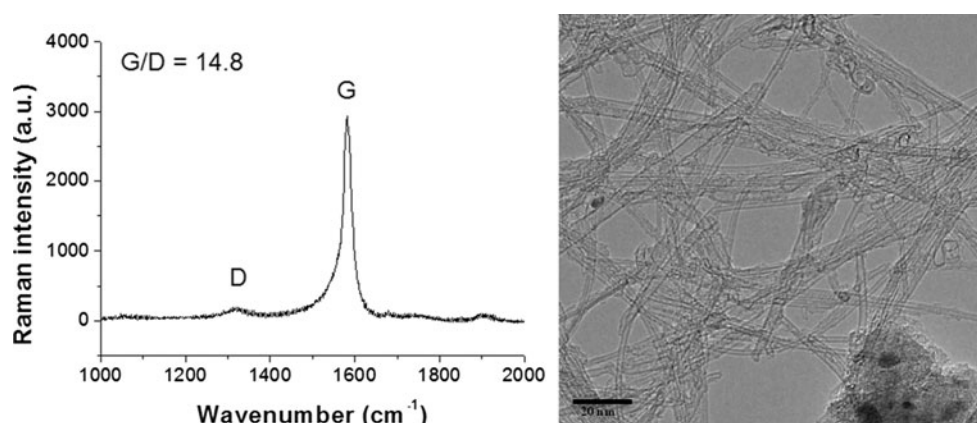
3.2.1 Catalyst Screening

A screening of different nanohybrids was conducted for the aldol-condensation of furfural and acetone. Since a basic catalyst is needed for this type of reactions, the activity of six different oxides (MgO, MgO/Al₂O₃, TiO₂, ZnO, Ce_xZr_{1-x}O₂ and V₂O₅) were compared. Therefore, they were first used as a support for the growth of SWCNT or MWCNT to produce the corresponding CNT/oxide nanohybrids.

Figure 5 compares the overall conversion of furfural and product yield in the aldol-condensation of furfural and acetone, after 3 h of reaction at 100 °C and 400 psi of N₂, over the different catalysts. It can be observed that the most active nanohybrids for the aldol-condensation reaction were the ones containing MgO (i.e., MWCNT/MgO, MWCNT/MgO/Al₂O₃ and SWCNT/MgO), with conversion values of up to 16%. The nanohybrids of MWCNT/TiO₂ exhibited some activity, but the ones containing ZnO, Ce_xZr_{1-x}O₂ and V₂O₅ led to conversion values lower than 1%.

The main product observed in all the cases was 4-(2-furyl)-3-buten-2-one (C₈), while small amounts of 2-furancarboxylic 2-furanmethyl ester (C₁₀) and 1,5-bis-(2-furanyl)-1,4-pentadien-3-one (C₁₃) were detected. The reaction pathways that explain the formation of these products are summarized in Scheme 1. The C₈ product results from the cross condensation of furfural and acetone. This molecule has an alpha H that allows it to make an additional condensation step, resulting in the double condensation product, 1,5-bis-(2-furanyl)-1,

Fig. 2 Raman spectrum (left) and HRTEM image (right) of the nanohybrids composed of SWCNT and MgO



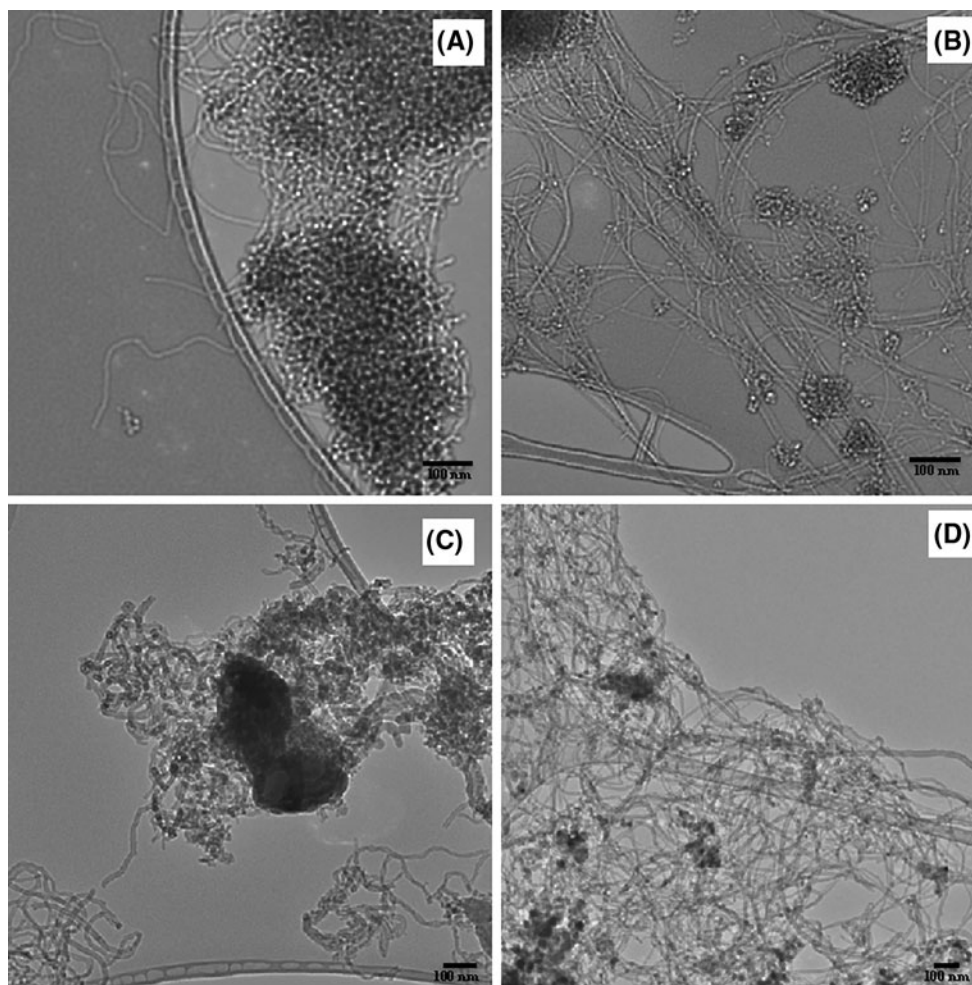
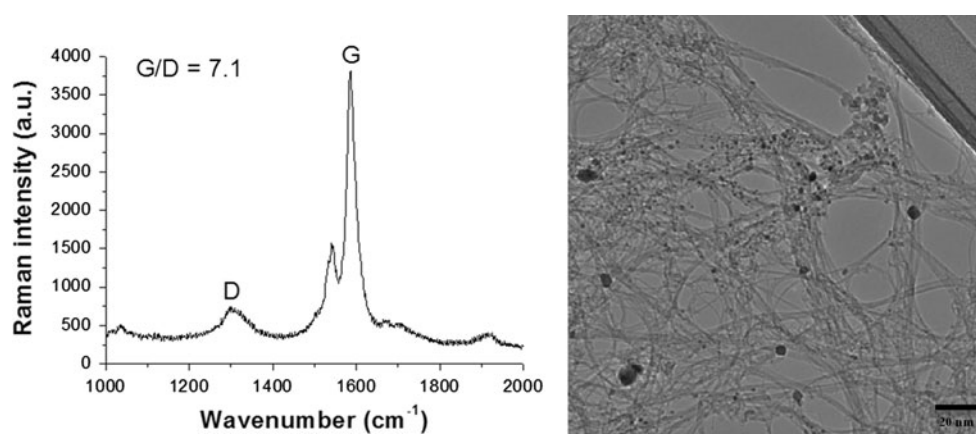


Fig. 3 HRTEM images of some of the nanohybrids used in this study: **a** MWCNT/MgO, **b** MWCNT/ MgO₂Al₂O₃, **c** MWCNT/ ZnO, and **d** MWCNT/ TiO₂

Fig. 4 *Left* Raman spectrum of the purified SWCNT, *right* HRTEM image of the catalyst of 10 wt% Pd on purified SWCNT



4-pentadien-3-one (C₁₃). Additionally, MgO in aqueous media also catalyzes the formation of the intermediate species for the Cannizzaro reaction [49–51]. That is, two molecules of

furfural can disproportionate into one of furoic acid and one of furfuryl alcohol, which later react to form the observed esterification product, 2-furancarboxylic 2-furanmethyl ester (C₁₀).

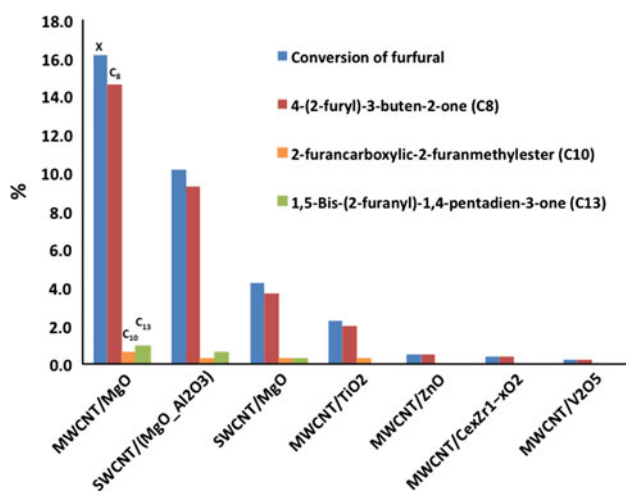
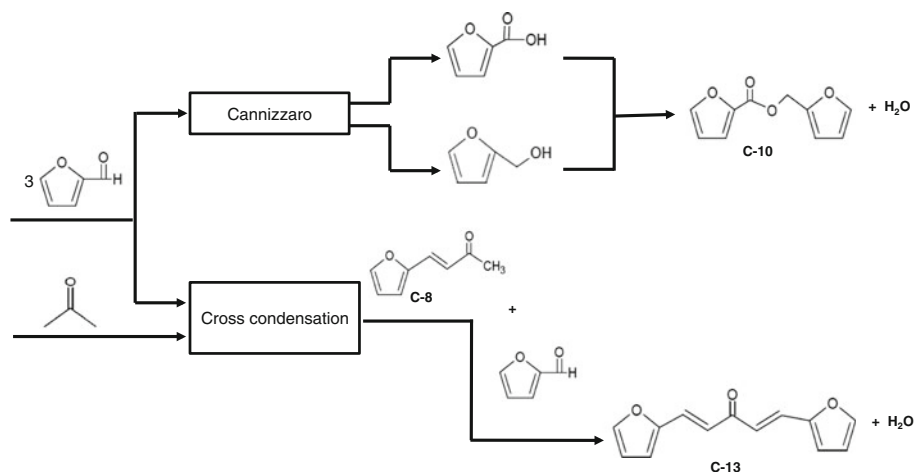


Fig. 5 Conversion of furfural and product yields (%) in the aldol-condensation of furfural and acetone over different nanohybrids for 3 h at 100°C and 400 psi of N₂. Feed: total molar concentration (furfural + acetone) of 1.8 M; furfural/acetone ratio of 1:5

As expected, products derived from self-condensation of acetone were not observed since this is always lower than the ketone-aldehyde cross-coupling [52]. Based on the results of this screening, the rest of the studies have focused on the aldol-condensation catalyzed by nanohybrids containing MgO, and both SWCNT and MWCNT.

It is worth noting the resistance to leaching exhibited by the nanohybrids after the high temperature calcination and nanotube growth procedure compared to untreated MgO. That is, when fresh MgO was added to water, it rapidly hydrolyzed to Mg(OH)₂ and a drastic change in pH was observed as it leached into the solution. However, when the nanohybrids composed of CNT fused to pre-calcined MgO were exposed to water, a negligible amount of MgO (less than 0.1 wt%) leached into the solution, as determined from the change in pH.

Scheme 1 Mechanism of the condensation reactions of furfural and acetone over CNT/MgO nanohybrids



3.2.2 Aldol-Condensation Reactions Over CNT/MgO

3.2.2.1 Single Phase Versus Emulsion System Comparison The aldol-condensation of furfural and acetone was studied in a single aqueous phase and in a water/decalin emulsion. The reaction in single phase was catalyzed by suspended MgO powder. For the reaction in emulsion, SWCNT/MgO nanohybrids located at the water/oil interface were used as both emulsifiers and catalysts. Figure 6 shows the molar yield of the three main products, 4-(2-furyl)-3-buten-2-one (C₈), 2-furancarboxylic 2-furanmethyl ester (C₁₀) and 1,5-bis-(2-furanyl)-1,4-pentadien-3-one (C₁₃), after 13 h in the batch reactor for the two systems.

It can be seen that the conversion was significantly higher in the biphasic emulsion than in the single liquid phase. It is worth noting that the single phase system resulted in almost no esterification products, i.e., 2-furancarboxylic 2-furanmethyl ester (C₁₀). Also, the yield of double condensation product 1,5-bis-(2-furanyl)-1,4-pentadien-3-one (C₁₃) in single phase was very small compared to the high production obtained in the emulsion system. The higher activity towards formation of long-chain molecules in the emulsion system could be attributed to a higher extent of dispersion of the suspended catalyst particles and a larger interfacial area [26, 28].

3.2.2.2 Time Evolution of Reaction in the Emulsion System Figure 7 shows the time evolution of conversion and product distribution at 100 °C and 400 psi N₂ in the batch reactor containing a water/oil emulsion catalyzed by MWCNT/MgO at a furfural/acetone ratio of 1:5. The main product for the conversion range investigated was C₈, from the direct cross-condensation of acetone and furfural, but its yield decreased with time due to further conversion to the C₁₃ double condensation product (see Scheme 1).

Figure 8 shows the time evolution of conversion when using SWCNT/MgO nanohybrids as a catalyst. A

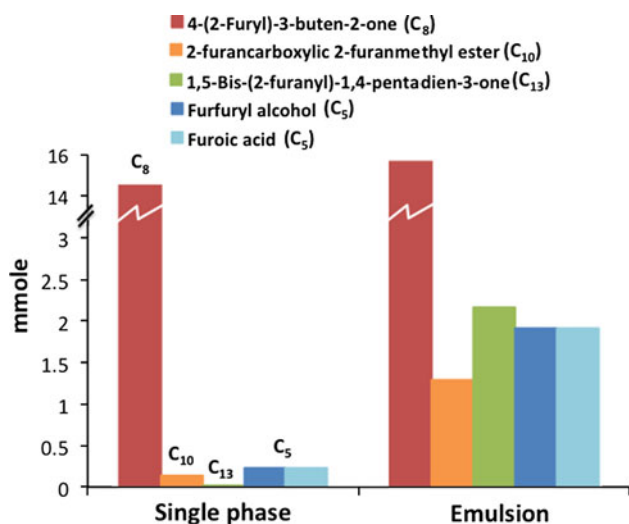


Fig. 6 Moles of products from the aldol-condensation of furfural and acetone in single phase (catalyst: MgO) and bi-phasic emulsion (catalyst: SWCNT/MgO). Reaction conditions: 13 h at 80 °C and 300 psi of He. Feed: total molar concentration (furfural + acetone) of 1.8 M; furfural/acetone ratio: 5:1

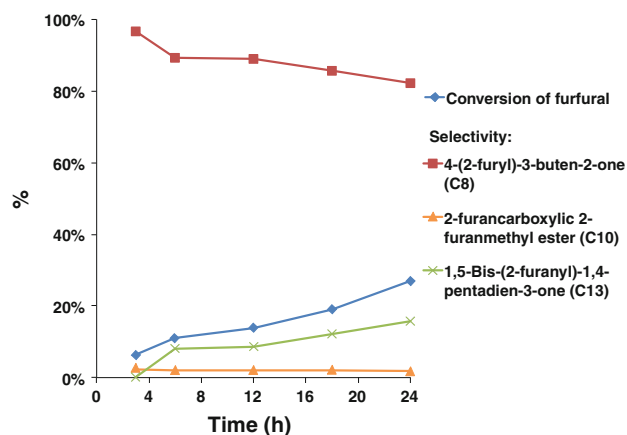


Fig. 7 Conversion of furfural and product selectivity (%) in the aldol-condensation of furfural and acetone over MWCNT/MgO nano hybrids at 100 °C and 400 psi of N₂. Feed: total molar concentration (furfural + acetone) of 1.8 M; furfural/acetone molar ratio of 1:5

pronounced change in product selectivity was observed as shown in Fig. 9; the selectivity of the direct cross-condensation product (C₈) decreased from about 66% to about 40% from 3 to 24 h, respectively, as it was consumed to form the double condensation product (C₁₃). The products of the Cannizzaro reaction [53], furfuryl alcohol and furoic acid, quickly react to form the 2-furancarboxylic 2-furanmethyl ester (C₁₀); therefore, their concentration remains relatively low, and keeping a molar ratio of 1:1 at all times, which is consistent with both their equimolar formation via Cannizzaro and their equimolar consumption via esterification.

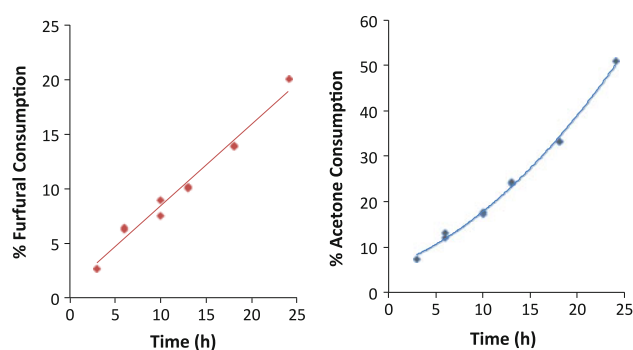


Fig. 8 Furfural and acetone consumption in the aldol-condensation reaction of acetone and furfural over SWCNT/MgO at 80 °C and 300 psi of He. Feed: total molar concentration (furfural + acetone) of 1.8 M; furfural/acetone molar ratio of 5:1

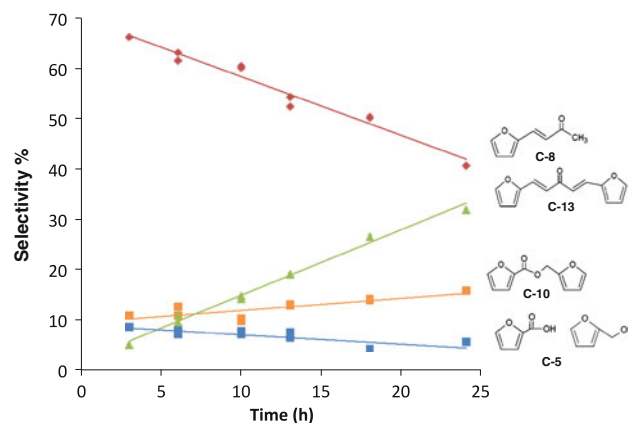
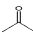
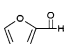
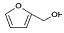
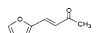



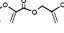
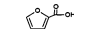
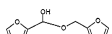




Fig. 9 Product selectivity from aldol-condensation reaction of acetone and furfural over SWCNT/MgO at 80 °C and 300 psi of He. Feed: total molar concentration (furfural + acetone) of 1.8 M; furfural/acetone molar ratio of 5:1

3.2.2.3 Partition of the Products Among the Three Phases Table 1 summarizes the distribution of the components from the feed and products among the three phases formed (i.e., light organic, aqueous, and heavy organic) after 10 h in the batch reactor with a furfural/acetone feed (molar ratio 5:1), at 80 °C, and 300 psi under He with SWCNT/MgO nano hybrid catalysts. It can be noticed that, before reaction, acetone and furfural distribute among the three phases. While furfural is enriched in the heavy organic phase, it also shows a significant concentration in the aqueous phase, where acetone is preferentially present.

After the aldol-condensation reaction, which takes place at the interface of the two phases, the direct condensation product (C₈) distributes among the phases, but the presence of the furfural greatly favors its solubility in the heavy organic phase. Due to their polarity and their affinity to furfural, the products of the Cannizzaro reaction (furfuryl alcohol, furoic acid, and 2-furancarboxylic 2-furanmethyl ester (C₁₀)) were not found in the light organic phase, but only in the aqueous and heavy organic phases. By contrast,

Table 1 Final product distribution of the aldol-condensation and aldol-condensation/hydrogenation reactions of furfural and acetone in a biphasic emulsion system

mmole Compound	Feed				Aldolcondensation				Hydrogenation			
	Aqueous	Organic	Heavy	Total	Aqueous	Organic	Heavy	Total	Aqueous	Organic	Heavy	Total
	12.2	2.3	6.0	20.5	8.0	0.6	1.6	10.2	3.3	0.2	0.7	4.2
	13.7	6.1	80.4	100.2	34.8	7.1	31.7	73.6	15.1	3.9	27.0	46.0
	–	–	–	–	0.9	–	0.2	1.1	2.4	0.6	2.5	5.5
	–	–	–	–	1.0	1.1	5.4	7.5	–	0.8	3.7	4.5
	–	–	–	–	–	–	–	–	–	2.5	0.4	2.9
	–	–	–	–	–	–	–	–	0.4	–	0.1	0.5
	–	–	–	–	1.3	–	0.1	1.5	2.5	–	0.5	3.0
	–	–	–	–	0.9	–	0.2	1.1	1.1	0.0	0.0	1.1
	–	–	–	–	–	–	–	–	2.0	–	2.0	2.2
	–	–	–	–	–	2.8	0.2	3.0	0.0	2.2	0.0	2.2
	–	–	–	–	–	–	–	–	–	3.1	0.3	3.4
	–	–	–	–	–	–	–	–	0.2	–	0.2	0.4
Carbon balance	100.0%				92.8%				83.4%			

Catalysts: SWCNT/MgO for aldol-condensation, and a physical mixture (wt. ratio 2:1) of SWCNT/MgO nanohybrids and 10 wt% Pd/Purified SWCNT for hydrogenation. Reaction conditions were 10 h at 80 °C in 300 psi of He for the aldol-condensation reaction and then 17 h at 100 °C in 300 psi of H₂ for the hydrogenation reaction

Feed: total molar concentration (furfural + acetone) of 1.8 M; furfural/acetone molar ratio of 5:1

the double condensation product (C₁₃) is not soluble in water and was mainly found in the light organic phase. These results illustrate the possibility of combining the conversion with product separation in a reaction single system.

3.3 Hydrogenation Reactions

3.3.1 MgO Nanohybrids-Catalyzed Aldol-Condensation Reactions Combined with Hydrogenation on Metallized Nanohybrids

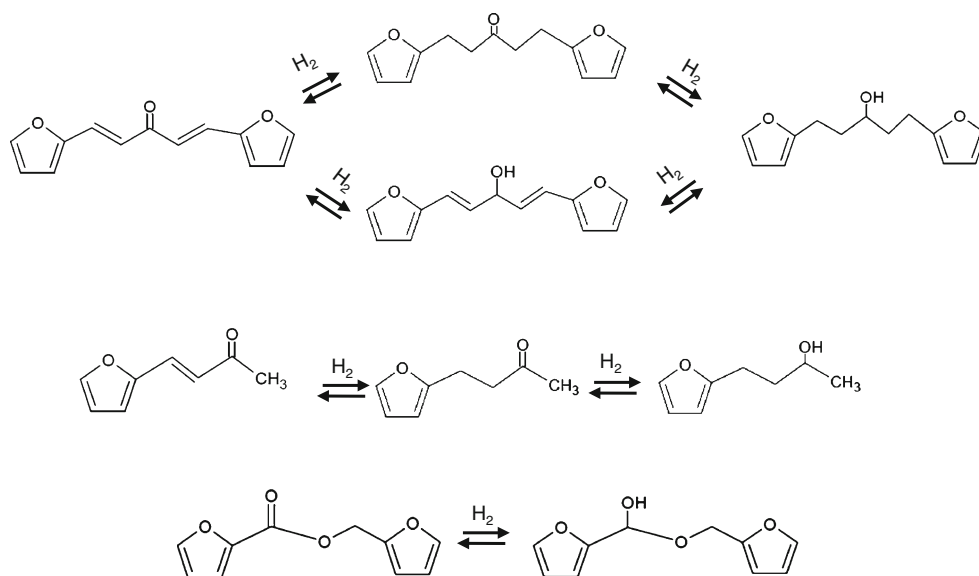
After the aldol-condensation of furfural and acetone, the hydrogenation of the condensation products was carried out using a physical mixture of SWCNT/MgO nanohybrids and 10 wt% Pd/Purified SWCNT (wt ratio 2:1). With this mixture, the former are used to stabilize the emulsion and catalyze the aldol-condensation reaction while the latter catalyze hydrogenation of the aldol-condensation products. Since in this case, all of the molecules generally partition among the aqueous and organic phases, a high phase-selectivity cannot be observed, as seen with molecules with larger solubility differences [26, 28, 29].

The results obtained after an initial 17 h of aldol-condensation followed by 10 h of hydrogenation are included in Table 1. Scheme 2 summarizes the possible products obtained from hydrogenation of the condensation products. Hydrogenation of the unsaturated ketones produces the corresponding furanyl alkyl ketone and alcohol, while hydrogenation of the ester compound yields the alkoxide hydroxyl derivative. These products were obtained and found distributed in the three phases according to their relative solubility.

As summarized in Table 1, 1,5-bis-2-furanyl-1,4-pentadien-3-one (C₁₃) was mostly present in the light organic phase and its first-step hydrogenation product, 1,5-bis-2-furanyl-penta-3-one was distributed in the light and heavy organic phases. However, when it was further hydrogenated, the resulting alcohol started to appear in the aqueous phase. After longer hydrogenation times, the 2-furancarboxylic 2-furanmethyl ester (C₁₀) was partially converted to 2-furanmethanol α -(2-furanylmethoxy). These compounds were not observed in the light organic phase, but in the aqueous and heavy organic phases.

After the aldol-condensation reaction, 4-(2-furanyl)-3-buten-2-one (C₈) was produced in a relative large amount

Scheme 2 Hydrogenation products from the C₈, C₁₀, and C₁₃ condensation compounds



and it was distributed among the three phases, but enriched preferentially in the heavy organic phase. After hydrogenation, this compound was partially hydrogenated to 4-(2-furanyl) butanone and 4-(2-furanyl) butan-2-ol. The former was primarily present in the light organic phase, while only a very small fraction was detected in the heavy organic layer. By contrast, the latter migrated almost entirely to the aqueous phase due to the high water affinity provided by the hydroxyl group in this secondary hydrogenation product, with only a very small amount moving to the heavy organic layer. These results illustrate the concept of using bifunctional nanohybrids to simultaneously convert and separate short oxygenates in a biphasic liquid into hydrogenated compounds of C chain length of interest for fuels.

3.3.2 NaOH-Catalyzed Aldol-Condensation Reactions Combined with Hydrogenation on Metallized Nanohybrids

To evaluate the use of solid nanohybrids in combination with a homogeneous basic catalyst, we used a strong base, NaOH (0.05 mol NaOH/mol furfural), to catalyze the initial aldol-condensation reaction. The resulting product distribution was significantly different from that obtained using the MgO-based nanohybrids (Fig. 10). With NaOH, a very high selectivity to the double condensation product (C₁₃) was obtained (>95%) at a furfural conversion of 7.3%. By contrast, the Cannizzaro reaction products were not observed with NaOH system since NaOH acts more as a base than as a nucleophile, favoring the aldol-condensation reaction [54].

Additionally, using NaOH, feeding furfural and acetone in a molar ratio of 2 and operating the system at 40 °C and 300 psi of He (Table 2), almost complete conversion of

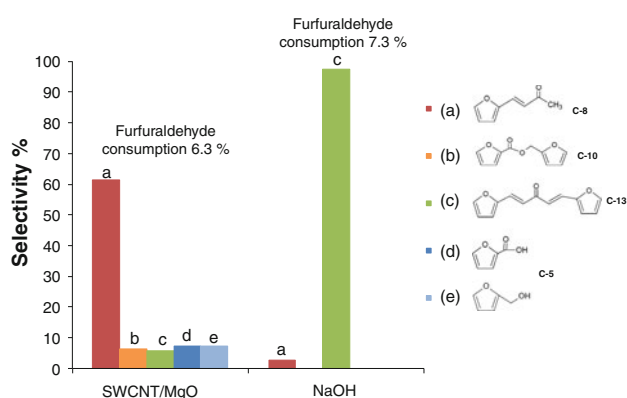
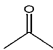
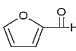
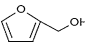
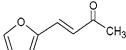
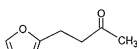
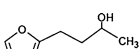
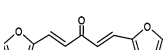
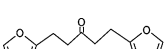
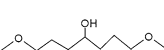
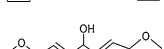


Fig. 10 Products distribution after 6 h reaction of acetone and furfural using NaOH (0.05 mol NaOH/mol furfural) and SWCNT/MgO nanohybrids at 80 °C and 300 psi of He. Feed: total molar concentration (furfural + acetone) of 1.8 M; furfural/acetone molar ratio of 2:1

acetone and furfural was observed (~100 and 94%, respectively). The major product from this reaction was the double condensation product (C₁₃), with a yield of 92%.

After the aldol-condensation reaction with NaOH, a hydrogenation reaction step catalyzed by Pt-functionalized nanohybrids (5 wt% Pt/MWCNT-Al₂O₃) was conducted in the same system, for 2 h at 100 °C and 800 psi of H₂, followed by 1 h at 230 °C and 900 psi of H₂. Table 2 shows that, during the hydrogenation, the cross-condensation product (C₈) was converted to the saturated ketone 4-(2-furanyl) butanone and subsequently to the corresponding alcohol, 4-(2-furanyl) butan-2-ol. Simultaneously, the double condensation product (C₁₃) was also hydrogenated to produce, in decreasing order, 1,5-bis-2-furanyl-penta-3-one, 1,5-bis-2-furanyl-pentan-3-ol and 1,5-bis-2-furanyl-1,4-pentadien-3-ol. It is also worth noting

Table 2 Final product distribution of the condensation/hydrogenation reaction of furfural and acetone

mmole Compound	Feed	Aldol-condensation reaction			Hydrotreating reaction		
		Catalyst NaOH	T (°C) 1 h at 40	P/He (psig) 300	Catalyst Al ₂ O ₃ (5% wt. Pt)	T (°C) 2 h at 100 1 h at 230	P/He (psig) 800 900
	22.5	0.0			0.0		
	45.0	2.6			0.0		
	–	0.0			2.5		
	–	0.7			0.0		
	–	0.0			0.3		
	–	0.0			0.4		
	–	19.5			0.0		
	–	0.0			11.5		
	–	0.0			7.6		
	–	0.0			0.2		
Carbon balance	100.0%	93.1%			91.8%		

Condensation was done for 1 h using 0.05 mol NaOH/mol furfural at 40 °C and 300 psi of He. Hydrogenation reaction was carried out with Pt functionalized nano-hybrids, 2 h at 100 °C and 800 psi of H₂, followed by 1 h at 230 °C and 900 psi of H₂

Feed: total molar concentration (furfural + acetone) of 1.8 M; furfural/acetone molar ratio of 2:1

that a small yield to tridecane and tridecanol was obtained in this reaction (<1%), which indicates that higher temperatures may be required for further deoxygenation.

3.4 Conversion of Synthetic Bio-oils

In order to further explore the effectiveness of this system with a more realistic feed, three different SBO were prepared and used as feed for the aldol-condensation and hydrogenation/hydrodeoxygenation reactions. The composition of the different synthetic bio-oils is summarized in Table 3. The SBO #1 and 2 were mainly composed of short oxygenates, with one of them containing acetic acid and the other not. SBO #3 was mainly a mixture of phenolic compounds.

3.4.1 Aldol-Condensation and Hydrogenation Reactions

The performance of MWCNT/MgO and MWCNT/ZnO nano-hybrids was compared for condensation and

hydrogenation of SBO #1 (with acid) and SBO #2 (without acid) (Table 3). The total yield, product yield, and total carbon balance are reported in Table 4. It can be noted that the yield of aldol-condensation products was low with both catalysts when using the SBO # 1 feed, with the overall conversion reaching values of less than 3% (Reactions #1 and #2 for the two catalysts). However, when using the SBO #2 feed the overall conversion reached 13.7% over MWCNT/MgO (Reaction #5). The reactivity of the ZnO nano-hybrids was low, even without acetic acid in the feed (Reaction #4, 1.9% conversion). Such decrease in performance of the MgO catalyst when acetic acid is present is certainly due to the strong chemisorption of acetic acid on the basic sites of MgO, which deactivates the catalyst rapidly.

From the known relative activities of oxygenates, one can expect that the major products arise from the self-condensation of propanal and the cross-coupling of furfurals and acetone (i.e., 2-methyl-pentanol (1c), 4-(2-furyl)-3-buten-2-one (4c) and 4-(furan-2-yl)-1-hydroxybut-3-en-2-one (3c)), as

Table 3 Composition (mol/L) of the different synthetic bio-oils prepared

Component	SBO #1 (mol/L)	SBO #2 (mol/L)	SBO #3 (mol/L)
Acetone	1.00	1.00	–
Propanal	1.00	1.00	–
2-Furfural	2.00	2.00	–
Methanol	1.00	1.00	–
Acetic acid	1.30	–	–
Acetol	0.50	0.50	–
m-Anisaldehyde	–	–	0.50
m-Cresol	–	–	0.50
Anisol	–	–	0.50
Benzaldehyde	–	–	0.50
2-Methoxy-4-methyl phenol	–	–	0.30
Cathecol	–	–	0.10
Guaiacol	–	–	0.50
4-Hydroxy-3-methoxy benzyl alcohol	–	–	0.05
Vanillin	–	–	0.05
Phenol	–	–	0.10
4-Hydroxy benzaldehyde	–	–	0.05

summarized in the reaction pathways shown in Scheme 3. In addition, a secondary esterification reaction took place between the products of the Canizzaro reaction (Scheme 1), producing 2-furancarboxylic 2-furanmethyl ester (C₁₀). Hydrogenation was conducted after the aldol-condensation step with Pd and Ni-containing ZnO catalysts, with the latter metal showing a significantly higher activity (Reactions #3 and #6 in Table 4).

Table 4 Total yield, product yield and total carbon balance obtained in the aldol-condensation and hydrogenation reactions of synthetic bio-oils SBO #1 and #2 at 100 °C and 400 psi in a biphasic system of decalin/water with an aqueous/organic ratio = 1.0

Feed SBO #	Catalyst	Reaction time (h)		Total yield (%)	Yield (%)										Total carbon balance (%)	
		N ₂	H ₂		3g	2b	1b	1c	4c	4d	3c	3d	2d	4e		4f
1	MWCNT/ZnO	3	–	2.6	0.0	0.0	0.0	0.2	1.8	0.0	0.2	0.0	0.1	0.4	0.0	95.3
1	MWCNT/MgO	3	–	0.8	0.0	0.0	0.2	0.0	0.3	0.0	0.0	0.0	0.1	0.2	0.0	98.7
1	MWCNT/ZnO + 10% Pd/SWCNT	3	3	4.5	0.1	0.2	0.6	0.2	0.5	1.0	0.1	0.2	0.1	0.4	1.2	93.2
2	MWCNT/ZnO	3	–	1.9	0.0	0.0	0.2	0.0	1.1	0.0	0.3	0.0	0.1	0.1	0.0	92.8
2	MWCNT/MgO	3	–	13.7	0.0	0.0	0.6	2.5	8.3	0.0	1.6	0.0	0.7	0.0	0.0	98.5
2	MWCNT/ZnO +5% Ni/SWCNT	3	3	2.0	0.0	0.1	0.0	0.1	0.9	0.2	0.2	0.0	0.1	0.0	0.3	91.4

The molecules presented in the table are: isopropanol (3g), furfuryl alcohol (2b), 2-methyl-pentenaldehyde (1b), 2-methyl-pentanol (1c), 4-(2-furyl)-3-buten-2-one (4c), 4-(furan-2-yl)butan-2-ol (4d), 4-(furan-2-yl)-1-hydroxybut-3-en-2-one (3c), 4-(furan-2-yl)butan-1,2-diol (3d), 2-furancarboxylic 2-furanmethyl ester (2d), 1,5-bis-(2-furanyl)-1,4-pentadien-3-one (4e) and 1,5-di(furan-2-yl)pentan-3-one (4f)

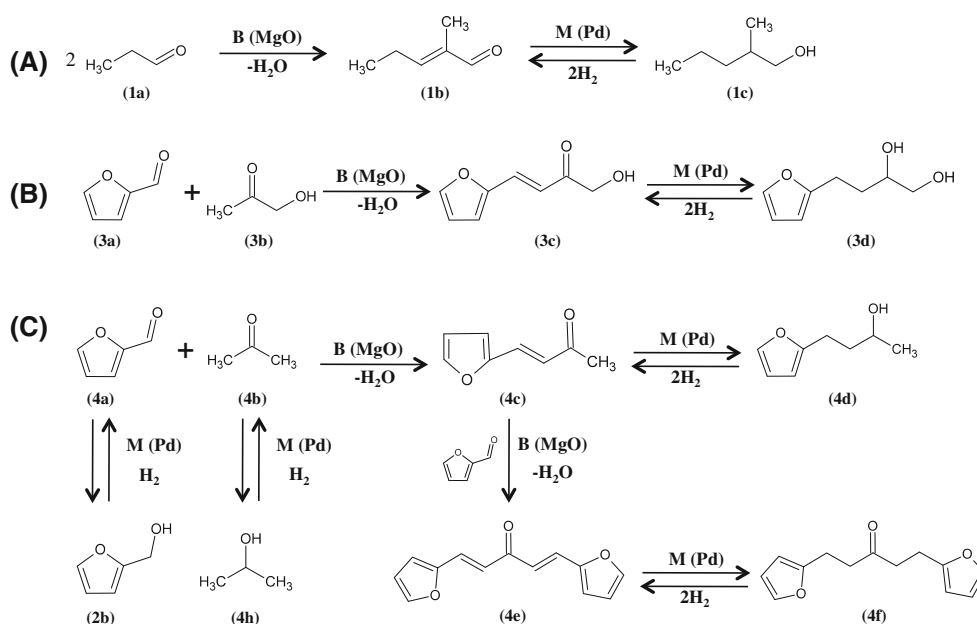
3.4.2 Hydrodeoxygenation of Phenolics Compounds

Partial hydrodeoxygenation of the SBO #3 was attempted at 100 °C and 400 psi of H₂ for 3 h over 5 wt% Pd/MWCNT/Al₂O₃. This synthetic bio-oil is a mixture of eleven different phenolic compounds with OH, methoxy ethers, and carbonyl groups. The possible reaction pathways are summarized in Scheme 4. The results of conversion, product yield, selectivity and carbon balance are reported in Table 5. The overall conversion was 49.2%, with benzyl alcohol and 4-hydroxybenzyl alcohol being the main products (with selectivities of 44.7 and 49.5%, respectively). As expected, under these mild reaction conditions, the aldehydes present in the feed were the only molecules that reacted to produce mainly the corresponding hydrogenation products (alcohols, 5b–8b) and to a lesser extent the hydrogenolysis products (deoxygenated phenolics, 6c–8c). While these cannot be considered fuel components, they should be stable enough for storage and transportation to a refinery where they could be incorporated into hydro-treating streams for full hydrodeoxygenation.

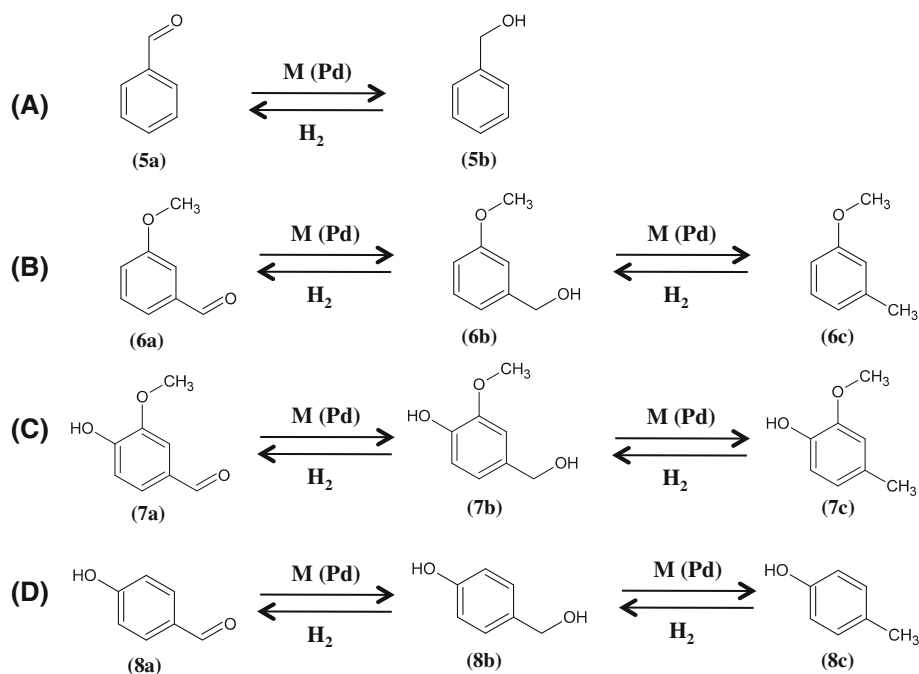
4 Conclusions

The following conclusions can be drawn from this study.

- (1) Amphiphilic nanohybrid catalysts can be effectively used to stabilize water/oil emulsions and conduct simultaneous condensation/hydrogenation reactions of biomass-derived oxygenates. The advantages of using this emulsion system include the enhancement of the mass transfer between phases due to a larger interfacial area, the possibility of maximizing the selective conversion of molecules present in each of



Scheme 3 Aldol-condensation and hydrogenation reactions of synthetic bio-oils SBO #1 and #2 at 100 °C and 400 psi in a biphasic system of decalin/water with an aqueous/organic ratio = 1.0



Scheme 4 Hydrodeoxygenation reaction of synthetic bio-oil SBO #3 at 100 °C and 400 psi of H₂ over 5 wt% Pd/MWCNT-Al₂O₃ in a biphasic system of decalin/water with an aqueous/organic ratio = 1.0

the phases (phase-selectivity), and the direct partitioning and separation of molecules based on differences in relative solubilities.

- (2) The aldol-condensation reaction of furfural and acetone is more effective in an emulsion system than in single aqueous phase. Furthermore, the presence of

the two phases in the emulsion facilitates the separation of the products.

- (3) The catalyst screening for the aldol-condensation reactions demonstrated that by tailoring the catalyst surface, one can improve the overall conversion. Among the different basic oxides employed to grow

Table 5 Conversion, product yields, selectivity and total carbon balance after 3 h of reaction of synthetic bio-oil SBO #3 over 5 wt% Pd/MWCNT-Al₂O₃ at 100 °C and 400 psi of H₂ in a biphasic system of decalin/water with an aqueous/organic ratio = 1.0

Component	Conversion (%)	Yield (%)	Selectivity (%)	Total carbon balance (%)
1-Methoxy-3-methylbenzene (6c)	49.2	0.2	0.3	98.1
Benzyl alcohol (5b)		22.0	44.7	
2-Methoxy-4-methylphenol (7c)		2.5	5.0	
<i>p</i> -Cresol (8c)		0.0	0.1	
3-Methoxybenzyl alcohol (6b)		24.4	49.5	
4-Hydroxybenzyl alcohol (8b)		0.2	0.4	

CNT on their surface, the nanohybrids supported on MgO have shown to be most effective for aldol-condensation. The main product is 4-(2-furanyl)-3-buten-2-one (C₈), which later reacts to produce the double condensation product 1,5-bis-(2-furanyl)-1,4-pentadien-3-one (C₁₃). In addition, the Canizzaro reaction is a side reaction in which, by the presence of OH groups, furfural undergoes disproportionation into the corresponding alcohol and acid. In turn, these products undergo esterification, which yields 2-furancarboxylic 2-furanmethyl ester (C₁₀). The selectivity to the longest-chain product (C₁₃) can be improved by using NaOH as a homogenous catalyst in the aqueous phase.

- (4) By incorporating active metals (Pd or Pt) onto the nanohybrids it is possible to hydrogenate the aldol-condensation products in the same emulsion system to more stable intermediate products. Alternative, fully deoxygenated long-chain alkanes (in this case tridecane) could be obtained by increasing the reaction temperature.
- (5) As a preliminary study of a more realistic feedstock, synthetic bio-oils were prepared and used as feed for the same type of reactions (aldol-condensation, hydrogenation and hydrodeoxygenation). Under the mild conditions employed for these reactions, we have been able to favorably convert the aldehydes present in the feed.

In summary, the presence of the two liquid phases with high interfacial area makes the conversion of the reactants and the separation of products more easily accomplished due to the differences in solubilities. This system presents many advantages and could have a major impact on the bio-fuels upgrading field.

Acknowledgment Funding was provided by NSF EPSCoR 0814361 and DoE EPSCOR (Grant DE-SC0004600). The authors also acknowledge SouthWest NanoTechnologies Inc. for providing some of the nanohybrids, and Mr. Anirudhan Gangadharan for preparing the ceria-zirconia mixed oxide.

References

1. Schmidt LD, Dauenhauer PJ (2007) *Nature* 447:914
2. Rostrup-Nielsen JR (2005) *Science* 308:1421
3. Somerville C, Youngs H, Taylor C, Davis SC, Long SP (2010) *Science* 329:790
4. US Department of Energy (2005) Feedstock Composition Gallery, Washington, DC.
5. Resasco DE (2011) *J Phys Chem Lett* 2:2294
6. Huber GW, Dumesic JA (2006) *Catal Today* 111:119
7. Bridgwater AV (1995) *Fuel* 14:631
8. Sutton D, Kelleher B, Ross JRH (2001) *Fuel Process Technol* 73:155
9. Mohan D, Pittman CU, Steele PH (2006) *Energy Fuels* 20:848
10. Demirbas A (2007) *Prog Energy Combust Sci* 33:1
11. Huber GW, Chheda JN, Barret CT, Dumesic JA (2005) *Science* 308:1446
12. Fakhfakh N, Cognet P, Cabassud M (2006) *J Soc Chim Tunis* 8:203
13. Fakhfakh N, Cognet P, Cabassud M, Luchesse Y, Dias de los Rios M (2008) *Chem Eng Process* 4:349
14. Barrett CJ, Chheda JN, Huber GW, Dumesic JA (2006) *Appl Catal B* 66:111
15. West RM, Liu ZY, Peter M, Gärtner CA, Dumesic JA (2008) *J Mol Catal A* 296:18
16. Shen W, Tompsett GA, Hammond KD, Xing R, Dogan F, Grey CP, Conner WC Jr, Auerbach SM, Huber GW (2011) *Appl Catal A* 392:57
17. Sádaba I, Ojeda M, Mariscal R, Fierro JLG, López Granados M (2011) *Appl Catal B* 101:638
18. Sádaba I, Ojeda M, Mariscal R, Richards R, López Granados M (2011) *Catal Today* 167:77
19. Choudary BM, Kantam ML, Sreekanth P, Bandopadhyay T, Figueras F, Tuel A (1999) *J Mol Catal A Chem* 142:361
20. Liu H, Peng L, Zhang T, Li Y (2003) *New J Chem* 27:1159
21. Lichtenthaler FW (2002) *Acc Chem Res* 35:728
22. Lewkowsky J, ARKIVOC (2001) 17
23. Piskorz J, Scott DS, Radlien D (1988) Composition of oils obtained by fast pyrolysis of different woods. In: Soltes J, Milne TA (eds) *Pyrolysis oils from biomass: producing analyzing and upgrading*. American Chemical Society, Washington, DC, pp 167–178
24. Czernik S, Bridgwater AV (2004) *Energy Fuels* 18:590
25. Peacocke GVC, Russel PA, Jenkins JD, Bridgwater AV (1994) *Biomass Bioenergy* 7:169
26. Crossley S, Faria J, Shen M, Resasco DE (2010) *Science* 327:68
27. Shen M, Resasco DE (2009) *Langmuir* 25:10843
28. Ruiz MP, Faria J, Shen M, Drexler S, Prasomsri T, Resasco DE (2010) *ChemSusChem* 4:964
29. Faria J, Ruiz MP, Resasco DE (2010) *Adv Synth Catal* 352:2359
30. Li XM, Reinhoudt D, Crego-Calama M (2007) *Chem Soc Rev* 36:1350
31. Zhang L, Resasco DE (2009) *Langmuir* 25:4792
32. Binks BP, Rodrigues JA (2005) *Angew Chem Int Ed* 44:441
33. Tambe DE, Sharma MM (1994) *Adv Colloid Interface Sci* 52:1
34. Bragg JR (1999) US Patent 5,855,243
35. Gangadharan A, Shen M, Sooknoil T, Resasco DE, Mallinson RG (2010) *Appl Catal A Gen* 385:80

36. Hori CE, Permana H, Simon Ng KY, Brenner A, More K, Rahmoeller KM, Belton D (1998) *Appl Catal B* 16:105
37. Noronha FB, Fendley EC, Soares RR, Alvarez WE, Resasco DE (2001) *Chem Eng J* 82:21
38. Santana RC, Do PT, Alvarez WE, Taylor JD, Sughrue EL, Resasco DE (2006) *Fuel* 85:643
39. Taylor J, McCormick R, Clark W (2004) Relationship between molecular structure and compression Ignition fuels, both conventional and HCCI. August 2004 NREL Report on the MP-540-36726, Non-Petroleum-Based Fuels
40. Do P, Crossley S, Santikunaporn M, Resasco DE (2007) Catalytic strategies for improving specific fuel properties. *Catalysis: specialist periodical reports*, vol 20. The Royal Society of Chemistry, London, p 33
41. Crossley S, Alvarez WE, Resasco DE (2008) *Energy Fuels* 22:2455
42. Jalali-Heravi M, Fatemi MH (2000) *J Chromatogr A* 897:227
43. Dillon AC, Yudasaka M, Dresselhaus MS (2004) *J Nanosci Nanotechnol* 4:691
44. Musumeci AW, Waclawik ER, Frost RL (2008) *Spectrochim Acta A* 71:140
45. Kobayashi Y, Takagi D, Ueno Y, Homma Y (2004) *Phys E* 24:26
46. Bachilo SM, Balzano L, Herrera JE, Pompeo F, Resasco DE, Weisman RB (2003) *J Am Chem Soc* 125:11186
47. Simpson JR, Fagan JA, Becker ML, Hobbie EK, Hight Walker AR (2009) *Carbon* 47:3238
48. Delhaes P, Couzi M, Trinquecoste M, Dentzer J, Hamidou H, Vix-Guterl C (2006) *Carbon* 44:3005
49. Peng XD, Barteau MA (1989) *Langmuir* 5:1051
50. Peng XD, Barteau MA (1992) *Catal Lett* 12:245
51. Keresszegi C, Ferri D, Mallat T, Baiker A (2005) *J Phys Chem B* 109:958
52. Solomons G, Fryhle C (1999) In: *Organic Chemistry*, 7th edn. Wiley, New York, p 1264
53. Wilson WC (1932) In: *Organic synthesis*, vol 1. Wiley, New York, p 269
54. Zeitsch KJ (2000) The chemistry and technology of furfural and its many by-products. *Sugar series*, 13. Elsevier, Amsterdam, p 159